Nature Environment and Pollution Technology
An International Quarterly Scientific Journal

p-ISSN: 0972-6268
(Print copies up to 2016)
e-ISSN: 2395-3454

Vol. 20 | No. 2 | pp. 775-783 | 2021

Original Research Paper

https://doi.org/10.46488/NEPT.2021.v20i02.039

Open Access Journal

Detection of Chromium(VI) in Water Using an Electrochemical Sensor Based on Ketjen Black-Modified Carbon Cloth

Yuxi Zhang*(**)(***), Xi Chen*†, Jingtao Liu* and Fengchun Yang****

*The Institute of Hydrogeology and Environmental Geology, Chinese Academy of Geological Sciences, Shijiazhuang 050061, China

**China University of Geosciences, Beijing 100083, China

***Key Laboratory of Groundwater Contamination and Remediation, China Geological Survey & Hebei Province, Shijiazhuang 050061, China

****Northwest University, Xi'an 710027, China

†Corresponding author: Xi Chen; mluzy_3335@163.com

Nat. Env. & Poll. Tech.
Website: www.neptjournal.com

Received: 30-04-2020
Revised: 18-06-2020
Accepted: 16-07-2020

Key Words:
Ketjen Black
Carbon cloth
Electrochemical sensor
Cr(VI)

ABSTRACT

A CB/CCE electrochemical sensor for Cr(VI) detection was prepared by ultrasonic dispersion of Ketjen Black and then the coating of modified carbon cloth electrode. Material morphology and composition were characterized based on XPS, TEM, BET, BJH; electrochemical performance of the electrode was studied based on LSV, EIS and CV. The results show that the high conductivity of Ketjen Black accelerates charge transfer on the electrode surface, while the abundant mesoporous structure and large specific surface area enhance Cr(VI) adsorption and reduction by the electrode. Under the optimal experimental conditions, the relationship between the reduction peak current of Cr(VI) and its concentration in the sample was studied by the i-t method. The reduction peak current intensity and its concentration demonstrate a good linear relationship in the range of 0.025-57μM and 57-483μM. The linear equations are: Ip(μA) = -0.2452C(μM)-0.0303 (R = 0.9908), Ip(μA) = -0.0329C(μM)-15.9212 (R = 0.9853), LOD is 9.88nM (S/N = 3). Compared with other methods, the sensor displays outstanding detection performance advantages. Plus the advantages of low cost and environmental protection, it has good application prospects in detecting Cr(VI) in water.

INTRODUCTION

Cr(VI), as one of the highly toxic ions, means strong carcinogenic risk to the human body (Jin et al. 2016). The increasingly serious Cr(VI) pollution in the water environment has greatly jeopardized water safety and the ecological environment. As an effective detection method for various metal ions, electrochemical detection has been greatly developed in the past decade (Zhang et al. 2014). Various electrode materials such as Au NPs, Ag/TiO_2 NPs/GCE, Fe_3O_4/MoS_2, NiFe/C/GCE have been used for detection of Cr(VI) in water (Ravindran et al. 2012, Zhang et al. 2016, Liu et al. 2017). However, metal nanomaterials feature complicated synthesis process, low stability and physiological toxicity, which limits their application in actual commercialization. Developing a non-metallic material with excellent electrocatalytic activity provides an effective way to overcome these problems (Dehghani et al. 2015). Some carbon nanomaterials with sp^2 hybrid structure, such as graphene (G), conductive carbon black (CB) and single-walled nanotubes (SWNTs), are regarded as the main candidates for non-metallic electrocatalysts. Electrode materials generally have abundant pore structure, numerous defect sites and high specific surface area, which facilitates the electrocatalytic process (Punckt et al. 2014). Recent studies have shown that mesopores (2-50 nm) act on the inner surface as ion transport channels, demonstrating high catalysis and low resistance (Kang et al. 2015). Hence, among the many candidates sp^2 hybrid carbon materials, carbon black with abundant mesopores and surface oxygen-containing functional groups undoubtedly displays a greater advantage.

Ketjen Black is carbon black made by a special process. Due to its stronger conductivity than ordinary conductive carbon black, its small addition will greatly improve battery quality and durability (Zhao et al. 2016). Its application is also common in high-end batteries, supercapacitors and many conductive and shielding materials. Carbon cloth (CC) is a conductive textile, which has received special attention as a flexible substrate due to its high specific surface area, electrical conductivity and chemical stability (Shao et al. 2017). CC features low cost, high resistance to damage, natural abundance and good mechanical properties, which

can greatly reduce the device integration difficulty while meeting the economic and high activity requirements of the sensor. Xu et al. (2017) constructed a new flexible non-enzymatic glucose electrochemical sensor using CC loaded with gold nanoparticles and polyaniline. Hai et al. (2015) used CC modified with NiAl layered double hydroxide for the electrochemical detection of glucose. Barsan (2012) reported that the use of CC modified with carbon nanotubes and nitrogen-doped carbon nanotubes resulted in a powerful biosensor. Although development based on CC electrode enjoys many applications in the medical and biological fields, its use is still relatively rare in the field of environmental detection.

In this study, an electrochemical sensor based on Ketjen black-modified carbon cloth electrode (CB/CCE) was prepared for the determination of Cr(VI) in water. The materials were characterized using X-ray photoelectron spectroscopy (XPS), Brunauer-Emmett-Teller (BET), Barrett-Joyner-Halenda (BJH), and transmission electron microscope (TEM). The electrochemical performance of the electrode was studied using linear sweep voltammetry (LSV), electrochemical impedance spectroscopy (EIS) and cyclic voltammetry (CV). The impact of experimental conditions was analysed, and the current concentration curve was obtained by the current-time method (i-t) to find the detection limit in the linear range. Finally, the electrode was checked for stability and anti-interference performance and successfully used in the detection of Cr(VI) in water samples.

MATERIALS AND METHODS

Reagents and Materials

Ketjen Black EC 300J, N, N-dimethylformamide (DMF) and $K_2Cr_2O_7$ (CP, 99%), graphene (900561-500MG) were procured from Sigma-Aldrich, Shanghai, China; carbon cloth was purchased from China Taiwan Carbon Energy Chemical Co. Ltd.; KCl, $K_3[Fe(CN)_6]$, $K_4[Fe(CN)_6]$, acetone, ethanol were purchased from Xi'an Jingbo Biotechnology Co. Ltd. Except for $K_2Cr_2O_7$, all other chemical reagents and electrochemical measuring reagents are of analytical grade without further purification.

The supporting electrolyte solution was 0.1M H_2SO_4-adjusted 0.1M Na_2SO_4 solution (pH=4.0); the analysis of electrochemical impedance chart was carried out in 0.1M KCl solution containing 5mM $[Fe(CN)_6]^{3-/4-}$. The solution was prepared using deionized water (18.3MΩ·cm) produced by the Millipore water purification system.

Electrode Modification

Before the experiment, the bare carbon cloth electrode was ultrasonically cleaned in acetone, ethanol, and secondary water for 15 minutes each, dried in a vacuum oven, and then cut into a small rectangle with a size of 1.0cm × 2.0cm for use. 1mg weighed Ketjen black nanoparticle sample was dispersed in 1 mL DMF solution, first undergoing ultrasonic dispersion in a low-frequency ultrasonic cleaner, and then sonication under a high-frequency ultrasonic instrument until ink-like Ketjen black dispersion liquid was formed, which was then evenly coated on the carbon cloth surface and baked under an infrared lamp to complete the modification.

Electrochemical Research

The composition of Ketjen black was analysed using XPS (ThermoFisher EscaLab 250Xi X-ray photoelectron spectrometer, USA), and its specific surface area and pore width were calculated using BET and BJH (Beishide 3H-2000PS1 static nitrogen adsorption specific area analyser, Beijing, China). Before measurement of N_2 adsorption isotherm, all test materials were degassed at 423 k for 12 hours. Morphology of the material was observed by TEM (transmission electron microscope FEI Tecnai G2 F30, USA).

All electrochemical measurement tools were provided by an electrochemical workstation (Chenhua CHI 660D, Shanghai, China). A conventional three-electrode system was used, including a carbon cloth electrode (1.0cm×2.0cm) as the working electrode, an Ag/AgCl electrode (saturated KCl) as the reference electrode, and a platinum wire as the auxiliary electrode.

Electrochemical impedance spectroscopy EIS was performed in the buffer under the same three-electrode configuration with a frequency range of 0.1~100000Hz and an AC probe amplitude of 50mV. Linear scanning voltammetry was carried out in Na_2SO_4 electrolyte solution at a sweep speed of $50mV \cdot s^{-1}$ and a scanning potential of -0.6~0.6V. The current-time method was performed in an electrolyte solution with a constant voltage of 0.1V and a pH of 4.0. Trace amount of Cr(VI) solution with fixed concentration was dropped into the magnetically stirred electrolyte solution every 50s. Record the i-t curve showing response current change with Cr(VI) concentration. All experiments were conducted at room temperature in the laboratory.

RESULTS AND DISCUSSION

Characterization of Materials

As shown in Fig. 1A, XPS analysis results clearly show that Ketjen Black is mainly composed of C and a small amount of O. Fig. 1B shows the C 1s peak of Ketjen Black, whose characteristic peaks are 284.6eV and 285.4eV, respectively, corresponding to C-C and C-O (Contarini et al. 1991). It

indicates that Ketjen Black almost has no heteroatoms and displays typical non-metallic properties.

Fig. 1 C and D are TEM images of Ketjen Black, which reflect its porous structure and pore size. There are various types of mesopores with different sizes and irregular shapes. The special porosity characteristics carry great significance for rapid charge transfer and accelerated reaction based on efficient use of internal structure.

In this study, Ketjen black was compared with other carbon nanomaterials graphene and single-walled carbon nanotubes in sp^2 hybrid orbital structure. Specific surface area and pore size distribution of the material were characterized by N_2 adsorption/desorption isotherm measurements. Fig. 2A shows different N_2 adsorption/desorption stages with linear single-layer/multi-layer adsorption properties, and hysteresis curves at relatively high pressures. The hysteresis loop has a relation with the capillary condensation process in the mesopore (Carrott et al. 1987). Compared to graphene and single-walled carbon nanotubes, Ketjen Black's Type IV isotherms exhibit a greater hysteresis loop, indicating the presence of more abundant mesopores (Liu et al. 2016). At the same time, under the relative pressure of 0.8~1.0, obvious macroporous absorption is shown on the Ketjen black surface. In addition, the Ketjen black pore size measured by the BJH method has a narrow mesopore

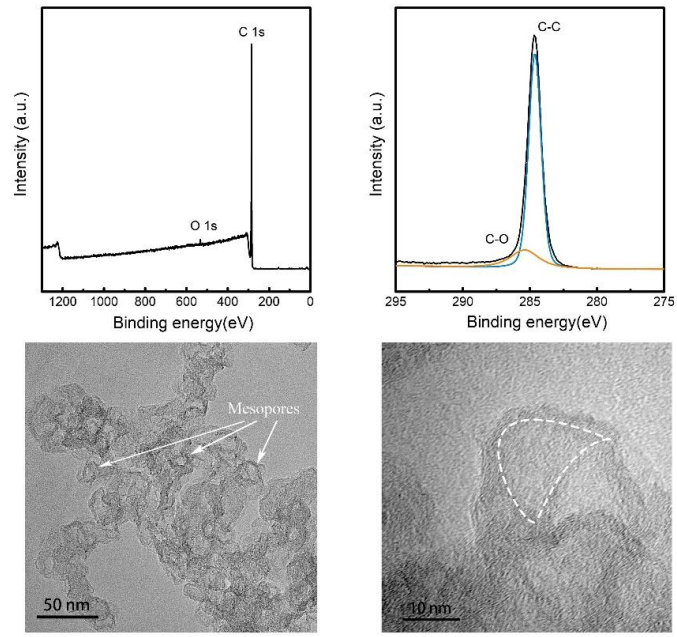

Fig. 1: (A)XPS analysis of CB. (B)High-resolution XPS analysis of the C 1s peak of CB. TEM characterizations of CB porous structure and size. Scale bars: 50nm (C); 10nm (D).

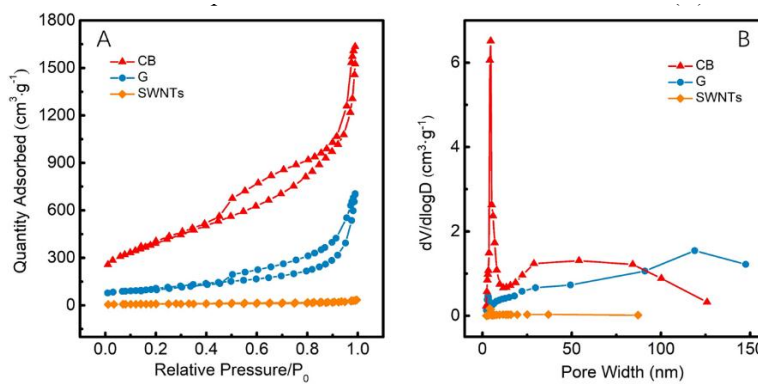

Fig. 2: Nitrogen adsorption-desorption isotherms (A) and pore size distribution by BJH method using the adsorption branch of isotherm (B) of CB, G and SWNTs.

Table 1: The surface area, pore volume and average pore diameter parameters of SWNTs, G and CB measured by the BET and BJH methods

Sample	BET Surface area ($m^2 \cdot g^{-1}$)	Total pore volume ($cm^3 \cdot g^{-1}$)	Average pore diameter (nm)
SWNTs	26.09	0.0403	6.17
G	328.69	0.8060	9.81
CB	1333.52	1.8528	5.56

distribution at around 5.56 nm (Fig. 2B), which facilitates the entry of accessible hydrated Cr(VI) into inner and outer pore surfaces during the rapid charge and discharge process.

Using BET and BJH methods, the relevant parameters of Ketjen Black are derived as given in Table 1. It shows that Ketjen Black has the largest specific surface area of $1333.52 m^2 \cdot g^{-1}$, the largest total pore volume of $1.8528 cm^3 \cdot g^{-1}$, and the smallest average pore size of 5.56nm. Specific surface area, pore size distribution and TEM images jointly prove that Ketjen Black has a rich mesoporous structure to provide an effective charge transfer channel for Cr(VI).

Electrochemical Performance of the Electrode

Fig. 3A shows the EIS diagram of CCE and modified CB/CCE in 5mM $[Fe(CN)_6]^{3-/4-}$ in 0.1M KCl. CB/CCE has a smaller semicircle diameter than CCE, indicating that CB/CCE has fast electron migration and great interface electron transfer between solution and interface material, which facilitates oxidation-reduction of iron ions on the working electrode while reducing the resistance value. CCE with great semicircle can promote oxidation-reduction of electrochemical probe iron, but with slow electron transfer. Ketjen Black with abundant mesoporous structures and the high surface area provides more active sites for the electrode reaction while improving the conductivity of the working electrode, facilitating charge transfer within the material, and accelerating charge transfer on the electrode surface, thus basically guaranteeing high sensitivity in Cr(VI) measurement.

To more directly investigate the increase in Ketjen Black electron migration rate, reduction peaks of CCE and CB/CCE were comparatively analysed by LSV. As shown in Fig. 3B, CCE has no obvious reduction peak in the range of -0.6~0.6V, while CB/CCB has a clear electrochemical reduction peak against Cr(VI) at a voltage of about 0.1V, indicating that CB has obvious electronic transfer.

CB on CCE played a significant catalytic role in the reduction of Cr(VI), demonstrating excellent electron conductivity. This is because CB with strong conductivity and great ion landing area has a strong absorption capacity against Cr(VI). The above results are consistent with EIS analysis conclusions, both indicating that the electrode surface with rich active sites and specific surface area can absorb and reduce Cr(VI) in large amounts. Hence, Ketjen Black displays outstanding performance in catalysing Cr(VI) and can significantly enhance the reduction of current strength against Cr(VI).

LSV was used to record the peak current response of the electrode during Cr(VI) concentration change from 1mM to 5mM. Fig. 4A shows that the reduction peak current increases with the increasing Cr(VI) concentration, exhibiting a good linear relationship. The linear regression equation is $I_p(\mu A) = -0.04826C(\mu M)-14.35$ ($R = 0.9987$) (Fig. 4B). Where, I_p represents the reduction peak current, and C represents Cr(VI) concentration. It also indicates Ketjen Black's excellent ability in reducing Cr(VI). Fig. 4C shows the logarithmic relationship between reduction peak current and peak voltage under different Cr(VI) concentrations. For a concentration as low as 1 mM, the peak current value and the peak voltage value remain almost unchanged at 0.11V. When the concentration varies between 1~5mM, a linear relation is shown between the logarithm of peak current and that of the peak voltage. In the reversible reaction, it is possible to predict the peak voltage value and electrolyte solution concentration in the experiment based on the above linear electrochemical

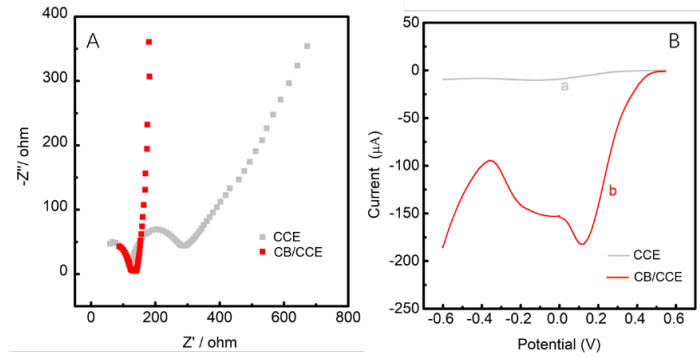

Fig. 3: (A) EIS of CCE and CB/CCE in a solution of 5mM $[Fe(CN)_6]^{3-/4-}$ in 0.1M KCl. (B) CCE(a) and CB/CCE(b) in 0.1M Na_2SO_4 (pH=4.0) of 5mM Cr(VI), Scan rate: $50 mVs^{-1}$.

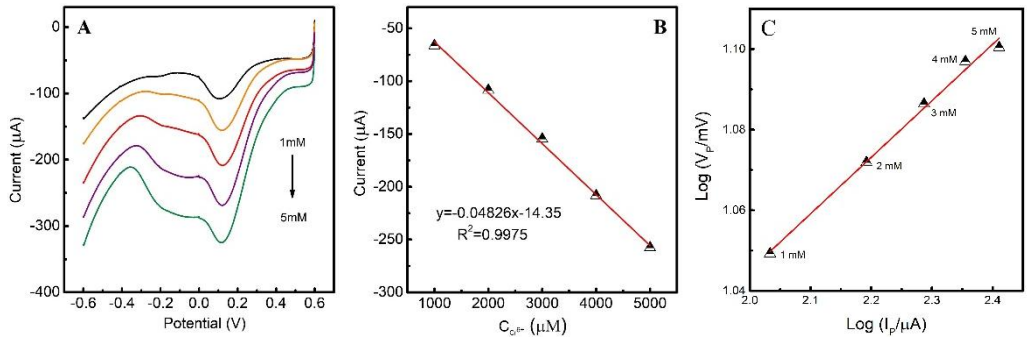

Fig. 4: (A) CV of Cr(VI) at Carbon black modified electrode in 0.1M Na_2SO_4 (pH = 4.0) when Cr(VI) concentrations are from 1mM to 5mM; (B) The plot of Ip versus Cr(VI) concentration; (C) Log(Vp/mV) vs Log(Ip/μA) for different concentration Cr(VI) .

model. If this model is not established, the reaction is an irreversible process. Hence, the electrode reaction here is a reversible process.

Fig. 5A shows that when the potential is set to -0.2~0.8V, changes in redox peak current in the test solution can be studied by changing sweep speeds so that kinetic properties can be analysed. As can be seen, redox has an increased response to current as the sweep speed increases from 10mV·s^{-1} to 130mV·s^{-1}, suggesting that CB/CCE has a good ability to reverse oxidation-reduction of iron ions. The peak current value in Fig. 5B has a good linear relationship with the square root of the sweep speed, and the corresponding peak current is proportional to the square root of the sweep speed. This indicates that an electrochemical process controlled by diffusion occurs on the modified electrode.

In this experiment, LSV was used to investigate the electrochemical behaviour of CB/CCE in the electrolyte solution with pH = 1.0~6.0. Fig. 6A shows the response of modified electrode to the electrochemical reduction current of 5mM Cr(VI) under different pH values. Obviously, in the voltage range of -0.6~0.6V, the electrochemical reduction current peak value of Cr(VI) increases as the pH value

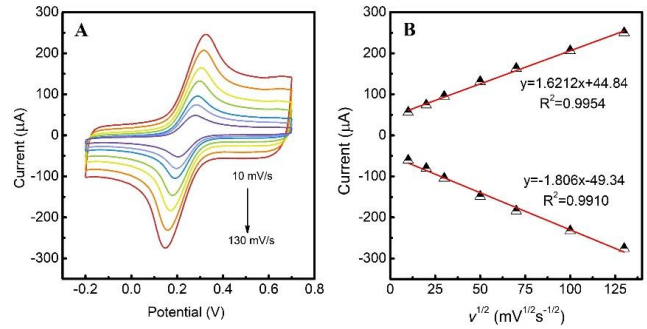

Fig. 5: (A) CVs of carbon black modified electrode in 0.1M Na_2SO_4 (pH = 4.0) with 0.5mM Cr(VI) at different scan rates of 10, 20, 30, 50, 70, 100, 130mVs^{-1}. (B) The plot of peak current versus the square root of scan rate.

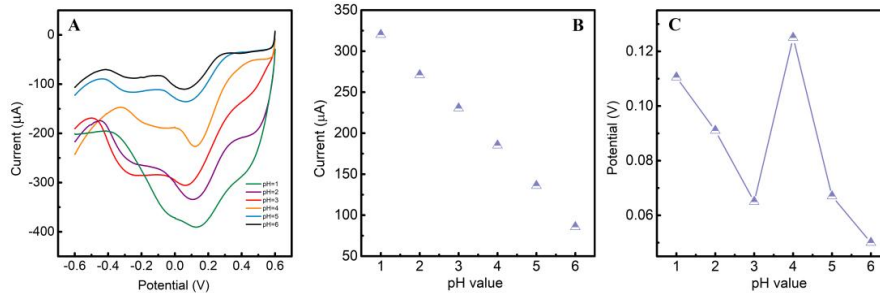

Fig. 6: (A) The current response of 5.0 mM Cr(VI) of different solution pH values; (B) The plot of current response for 5.0 mM Cr(VI) with the influence of solution pH; (C) the effect of potentials and pH value.

decreases. At low pH, Cr(VI) mainly exists in the form of $HCrO_4^-$. The electrostatic interaction between $HCrO_4^-$ and CB surface-functionalized with H^+ will facilitate Cr(VI) ion adsorption by CB in an acidic medium. Fig. 6B shows a significantly increased reduction current of Cr(VI) with increasing acidity. Fig. 6C reflects that in the corresponding relationship between the peak potential and different pH values, electrolyte solution with a pH value of 4.0 has the most positive potential when detecting Cr(VI).

Due to the extremely high H^+ conductivity in transferring electrons through hydrogen bonds, when the H^+ exponent in the solution increases exponentially, electrolyte solution has redoubled electron migration rate, so that Cr(VI) (0~0.2V) and Cr(III) (-0.1~0.3V) peaks continuously expand. At the same time, with the increasing acidity, a large reduction peak also appears at 0.4~0.6V. It is speculated that excessive Cr(VI) adsorbed on the Ketjen black material at the same time results in great changes in material structure and its electron transfer capacity so that saturation peak appears. When the solution has excessive acidity, the two impurity peaks even block the reduction peak of Cr(VI), making trace detection of Cr(VI) impossible. In view of the above reasons, it was finally decided to select pH 4.0 as the most appropriate pH value for Cr(VI) detection.

Linear Range and Detection Limit

The linear range of Cr(VI) detection by electrodes was studied by the i-t method. First, fix the potential at 0.12V, and add a certain amount of Cr(VI) in 40 mL electrolyte solution (pH=4.0) every 50 s, then record the response curve of current over time, as shown in Fig. 7A. The mosaic reveals that the current shows a clear response at the addition of the first drop of 0.025 μM Cr(VI). At the same time, the detection limit (LOD) is calculated to be 9.88 nM, S/N = 3 according to the calculation formula: LOD = $3S_y/m$. Where S_y is the standard deviation and m is the slope of the calibration curve.

Fig. 7B shows the calibration curve about the relationship between the current response of CB/CCE and Cr(VI) concentration. There is a good linear relationship between the two, and the two equations of linear regressions between the peak current value and Cr(VI) concentration are as follows:

$$Ip(\mu A) = -0.2452C(\mu M) - 0.0303 \quad (R=0.9908),\ (0.025\sim57\mu M) \qquad \ldots(1)$$

$$Ip(\mu A) = -0.0329C(\mu M) - 15.9212 \quad (R=0.9853),\ (57\sim483\mu M) \qquad \ldots(2)$$

The linear response range is 0.025~483 μM. Sensitivity calculated based on low concentration range is 0.25 $\mu A \mu M^{-1} \cdot cm^{-2}$. The good linear relationship also reflects the accurate and sensitive ability of CB/CCE in detecting Cr(VI). The two-stage linear phenomenon may be a result of the two electrochemical processes of diffusion and adsorption during the reaction. In the diffusion process, the current increases with the increasing concentration, while in the adsorption process, excessive molecules completely occupy the material, resulting in reduced removal efficiency. At the end of the reaction, the oxide is adsorbed on the electrode, reducing the effective area of the electrode and leading to lower resulting sensitivity.

Table 2 lists the comparison of Cr(VI) detection performance of sensors built herein and by other modified materials. It suggests that the electrode has a lower detection limit and a wider linear range.

Stability and Anti-Interference

First, electrode reproducibility was studied by current measurement. A total of 4 evaluations were performed,

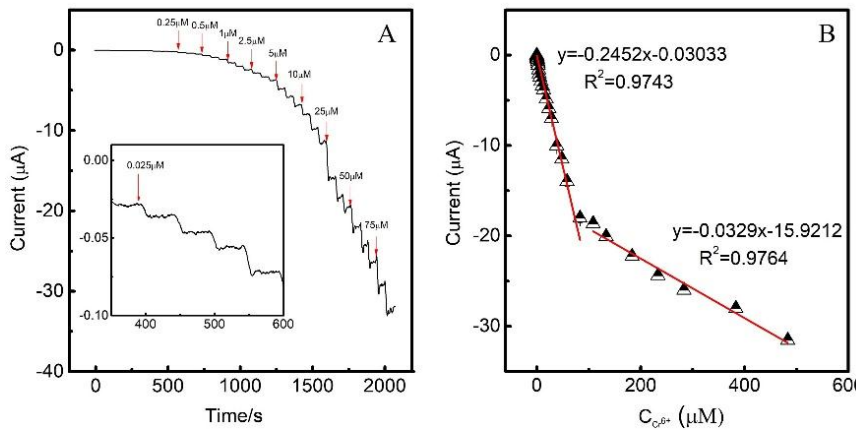

Fig. 7: (A) Various concentrations of Cr(VI) from 0.025 to 483μM in 0.1M Na_2SO_4 (pH = 4.0) at an applied potential of 0.12V. The lower concentrations were showed in the inset.(B) The calibration curve between the current and the concentration of Cr(VI).

Table 2: Comparison of quality parameters between Cr(VI) sensors developed in different literatures.

Electrode/surface	pH	Linear range (μM)	LOD (nM)	Reference
Ag/TiO_2 NPs/GCE	1.0	0.01~3.1	10	(Ravishankar et al. 2015)
Fe_3O_4/MoS_2	1.0	0.5~328	200	(Zhang et al. 2016)
NiFe/C/GCE	4.0	0.025~98.3	10	(Liu et al. 2017)
LMB/MB	2.0	10~500	100	(Sadeghi & Garmroodi 2013)
MWCNTs-SPCE	1.0	1~200	300	(Korshoj et al. 2015)
SPEs	1.0	3~10000	1000	(Miscoria et al. 2014)
PANI/GQDs	1.0	1.92~192	1865	(Punrat et al. 2016)
Ti/TiO_2NT/Au	1.0	0.1~105	30	(Jin et al. 2014)
Activated GCE	6.0	0.4~250	100	(Richtera et al. 2016)
BDD	1.0	0.192~96	57.7	(Fierro et al. 2012)
GCE/NF/Ag nano	2.0	0.38~4.42	12	(Xing et al. 2011)
Gold plated carbon	0.5	0.385~38.462	85	(Kachoosangi & Compton 2013)
PVC/POT/GCE	2.0	0.03~1.3	12	(Izadyar et al. 2016)
CB/CCE	4.0	0.025~483.2	9.88	This work

and the relative RSD was about 4.3% in the 4 test results, showing good test reproducibility. At the same time, before Cr(VI) addition, the current curves were static and balanced, demonstrating high electrode stability. According to the current response of the electrode towards 5 mM Cr(VI) for 7 consecutive days, the current response signal is 88% of the initial after 7 days, indicating good stability of the electrode.

Cr(VI) detection performance of the electrode was studied using the i-t method in the presence of common coexisting ions. First, Cr(VI) with a concentration of 10μM was added to 0.1M Na_2SO_4 (pH 4.0) solution. Afterwards, 1.0mM interfering ions K^+, Zn^{2+}, Mg^{2+}, Cu^{2+}, Ca^{2+}, Ni^{2+}, Fe^{2+}, Mn^{2+}, Pb^{2+}, Cl^- and SO_4^{2-} were added in succession. Finally, 10μM Cr(VI) was added. Fig. 8 indicates that the 10μM Cr(VI) added successively produces a current response of about 2μA, and the measurement current has insignificant changes after the addition of all interfering ions. That is, the fluctuation of interfering ions is extremely weak compared to Cr(VI). It suggests that the electrode still has extraordinary Cr(VI) detection performance in the presence of high-concentration interfering ions.

Sample Testing

To evaluate the performance of the built Cr(VI) electrochemical sensor in practical applications, real water samples were tested. The water sample was taken from a sewage outfall in an industrial park in Xi'an, China. After the sample filtration using a 0.45μm filter membrane, the pH value was adjusted to 4.0 using a buffer solution. Samples were detected by the "standard addition method", and ICP-AES test results were compared, as given in Table 3. It reveals that in real water sample detection, the sensor has a small relative standard deviation (2.3%~3.4%), a high recovery rate (98%~103%), and detection result consistent with ICP-AES, demonstrating the reliability of the sensor in actual detection.

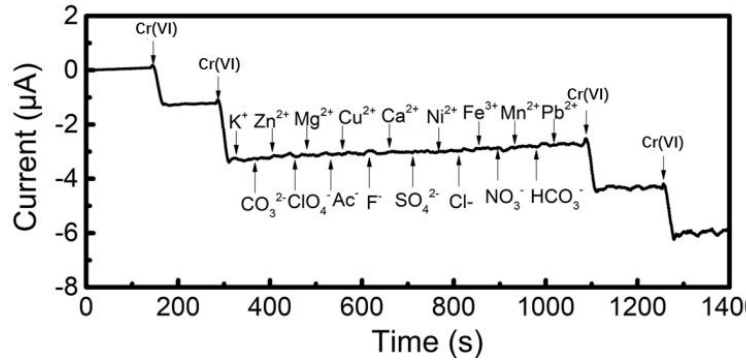

Fig. 8: Interference test of the sensor in 0.1M Na_2SO_4 (pH = 4.0) at 0.12V with 10μM Cr(VI) and 1.0mM other interferents as indicated

Table 3: Determination of Cr(VI) in the water sample using the standard addition method.

Sample	Added (μM)	Found (μM)	Determined (μM)	Recover (%)	RSD (n=3, %)	ICP-AES (μM)
1	10	10.57	0.58	98	3.1	0.57
	20	20.57		99	3.0	
	30	30.57		98	3.4	
2	10	11.08	1.06	102	2.6	1.02
	20	21.07		101	2.7	
	30	31.07		101	2.3	
3	10	12.63	5.47	103	3.0	5.48
	20	22.60		102	3.2	
	30	32.52		101	3.4	

CONCLUSION

A CB/CCE electrochemical sensor for Cr(VI) detection was prepared by ultrasonic dispersion of Ketjen Black and then a coating of modified carbon cloth electrode. The high conductivity of Ketjen Black accelerates the charge transfer on the electrode surface, and the abundant mesoporous structure and large specific surface area enhance Cr(VI) adsorption and reduction by the electrode. Under the optimal conditions, the linear range of Cr(VI) was determined to be 0.025~483μM using the i-t method, with two-step linear regression equations being Ip(μA) = -0.2452C(μM)-0.0303 (R = 0.9908), I_p(μA) = -0.0329C(μM)-15.9212 (R = 0.9853), and LOD is 9.88 nM, S/N = 3. The sensitivity was 0.25 μA $\mu M^{-1} \cdot cm^{-2}$ under the low concentration range. The sensor has been successfully used for testing Cr(VI) in actual water samples. In contrast with previous research reports, Ketjen black modified electrode not only has better ability in detecting Cr(VI) than other metal nanoparticle modified electrodes but also has microscopic advantages like abundant adsorption specific surface area, as well as macroscopic advantages of environmental protection, low cost and easy availability. At the same time, flexible carbon cloth substrate with low cost and high resistance to damage favours use in fieldwork.

ACKNOWLEDGEMENTS

The study was financially supported by projects of the China Geological Survey (No. DD20160308 and No. DD20190331).

REFERENCES

Barsan, M. M., Carvalho, R. C., Zhong, Y., Sun, X. and Brett, C. M. 2012. Carbon nanotube modified carbon cloth electrodes: Characterisation and application as biosensors. Electrochim. Acta, 85: 203-209.

Carrott, P., Roberts, R. A. and Sing, K. 1987. Adsorption of nitrogen by porous and non-porous carbons. Carbon, 25(1): 59-68.

Contarini, S., Howlett, S. P., Rizzo, C. and De Angelis, B. A. 1991. XPS study on the dispersion of carbon additives in silicon carbide powders. Appl. Surf. Sci., 51(3-4): 177-183.

Dehghani, M. H., Taher, M. M., Bajpai, A. K., Heibati, B., Tyagi, I., Asif, M., Agarwal, S. and Gupta, V. K. 2015. Removal of noxious Cr (VI) ions using single-walled carbon nanotubes and multi-walled carbon nanotubes. Chem. Eng. J., 279: 344-352.

Fierro, S., Watanabe, T., Akai, K. and Einaga, Y. 2012. Highly sensitive detection of Cr^{6+} on boron doped diamond electrodes. Electrochim. Acta, 82: 9-11.

Hai, B. and Zou, Y. 2015. Carbon cloth supported NiAl-layered double hydroxides for flexible application and highly sensitive electrochemical sensors. Sensor. Actuat. B-Chem., 208: 143-150.

Izadyar, A., Al-Amoody, F. and Arachchige, D. R. 2016. Ion transfer stripping voltammetry to detect nanomolar concentrations of Cr (VI) in drinking water. J. Electroanal. Chem., 782: 43-49.

Jin, W., Du, H., Zheng, S. and Zhang, Y. 2016. Electrochemical processes for the environmental remediation of toxic Cr (VI): A review. Electrochim. Acta, 191: 1044-1055.

Jin, W., Wu, G. and Chen, A. 2014. Sensitive and selective electrochemical detection of chromium (VI) based on gold nanoparticle-decorated titania nanotube arrays. Analyst, 139(1): 235-241.

Kachoosangi, R. T. and Compton, R. G. 2013. Voltammetric determination of Chromium (VI) using a gold film modified carbon composite electrode. Sensor. Actuat. B-Chem., 178: 555-562.

Kang, D., Liu, Q., Gu, J., Su, Y., Zhang, W. and Zhang, D. 2015. "Egg-Box"-assisted fabrication of porous carbon with small mesopores for high-rate electric double layer capacitors. ACS Nano, 9(11): 11225-11233.

Korshoj, L. E., Zaitouna, A. J. and Lai, R. Y. 2015. Methylene blue-mediated electrocatalytic detection of hexavalent chromium. Anal. Chem., 87(5): 2560-2564.

Liu, J., Ding, Y., Ji, L., Zhang, X., Yang, F., Wang, J. and Kang, W. 2017. Highly sensitive detection of Cr (VI) in groundwater by bimetallic NiFe nanoparticles. Anal. Methods-UK, 9(6): 1031-1037.

Liu, Y., Shi, Z., Gao, Y., An, W., Cao, Z. and Liu, J. 2016. Biomass-swelling assisted synthesis of hierarchical porous carbon fibers for supercapacitor electrodes. ACS Appl. Mater. Inter., 8(42): 28283-28290.

Miscoria, S. A., Jacq, C., Maeder, T. and Negri, R. M. 2014. Screen-printed electrodes for electroanalytical sensing, of chromium VI in strong acid media. Sensor. Actuat. B-Chem., 195: 294-302.

Punckt, C., Pope, M. A. and Aksay, I. A. 2014. High selectivity of porous graphene electrodes solely due to transport and pore depletion effects. J. Phys. Chem. C, 118(39): 22635-22642.

Punrat, E., Maksuk, C., Chuanuwatanakul, S., Wonsawat, W. and Chailapakul, O. 2016. Polyaniline/graphene quantum dot-modified screen-printed carbon electrode for the rapid determination of Cr(VI) using stopped-flow analysis coupled with voltammetric technique. Talanta, 150: 198-205.

Ravindran, A., Elavarasi, M., Prathna, T. C., Raichur, A. M., Chandrasekaran, N. and Mukherjee, A. 2012. Selective colorimetric detection of nanomolar Cr (VI) in aqueous solutions using unmodified silver nanoparticles. Sensor. Actuat. B-Chem., 166: 365-371.

Ravishankar, T. N., Muralikrishna, S., Nagaraju, G. and Ramakrishnappa, T. 2015. Electrochemical detection and photochemical detoxification of hexavalent chromium (Cr (VI)) by Ag doped TiO_2 nanoparticles. Anal. Methods-UK, 7(8): 3493-3499.

Richtera, L., Nguyen, H. V., Hynek, D., Kudr, J. and Adam, V. 2016. Electrochemical speciation analysis for simultaneous determination of Cr(III) and Cr(VI) using an activated glassy carbon electrode. Analyst, 141(19): 5577-5585.

Sadeghi, S. and Garmroodi, A. 2013. A highly sensitive and selective electrochemical sensor for determination of Cr(VI) in the presence of Cr(III) using modified multi-walled carbon nanotubes/quercetin screen-printed electrode. Mat. Sci. Eng. C-Mater, 33(8): 4972-4977.

Shao, X., Zheng, X., Zou, W., Luo, Y., Cen, Q., Ye, Q., Xu, X. and Wang, F. 2017. Alkali conversion of Ni-Co nanoarrays on carbon cloth for a high-capacity supercapacitor electrode. Electrochim. Acta, 248: 322-332.

Xing, S., Xu, H., Chen, J., Shi, G. and Jin, L. 2011. Nafion stabilized silver nanoparticles modified electrode and its application to Cr(VI) detection. J. Electroanal. Chem., 652(1-2): 60-65.

Xu, M., Song, Y., Ye, Y., Gong, C., Shen, Y., Wang, L. and Wang, L. 2017. A novel flexible electrochemical glucose sensor based on gold nanoparticles/polyaniline arrays/carbon cloth electrode. Sensor. Actuat. B-Chem, 252: 1187-1193.

Zhang, X., Yu, S., He, W., Uyama, H., Xie, Q., Zhang, L. and Yang, F. 2014. Electrochemical sensor based on carbon-supported $NiCoO_2$ nanoparticles for selective detection of ascorbic acid. Biosens. Bioelectron., 55: 446-451.

Zhang, Y., Chen, P., Wen, F., Yuan, B. and Wang, H. 2016. Fe_3O_4 nanospheres on MoS_2 nanoflake: Electrocatalysis and detection of Cr(VI) and nitrite. J. Electroanal. Chem., 761: 14-20.

Zhao, D., Qian, X., Jin, L., Yang, X., Wang, S., Shen, X., Yao, S., Rao, D., Zhou, Y. and Xi, X. 2016. Separator modified by Ketjen black for enhanced electrochemical performance of lithium-sulfur batteries. RSC Adv., 6(17): 13680-13685.